Articles

Optimization of Lithium Conductivity in La/Li Titanates

Ainhoa Morata-Orrantia, Susana García-Martín,* and Miguel Á. Alario-Franco

Departamento de Química Inorgánica, Facultad de Ciencias Químicas, Universidad Complutense, Madrid-28040, Spain

Received April 15, 2003. Revised Manuscript Received July 8, 2003

We have found that for the lanthanum/lithium titanates and related materials with a perovskite-related structure, ABO_3, optimum lithium conductivity takes place for a particular concentration of A-cation vacancies (□) equal to 8%. We have prepared a new oxide with the highest lithium conductivity reported to date for a crystalline material ($\sigma_{295\ K} = 2.95 \times 10^{-3}$ Scm^{-1}). This is $La_{0.56}Li_{0.36}\square_{0.08}Ti_{0.97}Al_{0.03}O_3$, the $x = 0.03$ composition in the solid solution of general formula $La_{0.56}Li_{0.33+x}\square_{0.11-x}Ti_{1-x}Al_xO_3$ ($0 \le x \le 0.06$). A similar situation is obtained for $x = 0.03$ in the related system $La_{0.56-x}Sr_xLi_{0.33+x}\ \square_{0.11-x}TiO_3$, where $\sigma_{295\ K} = 2.54 \times 10^{-3}$ Scm^{-1}. We have also prepared a material with the highest known conductivity ($\sigma_{295K} = 1.9 \times 10^{-3}$ Scm^{-1}) in the "classical" $La_{2/3-x}Li_{3x}\square_{1/3-2x}TiO_3$ system and it also corresponds to the same A-cation deficiency. Optimization of Li conductivity requires then both the control of the charge carriers/vacancies ratio as well as shortening of the B−O distances or increasing of the A−O distances. 3-D microtwinning is observed in the crystals of all these oxides, which have a $\approx\sqrt{2}a_p \times \approx\sqrt{2}a_p \times \approx 2a_p$ perovskite superstructure.

Introduction

The development of all-solid state batteries has mainly focused on polymer electrolytes despite their low ionic conductivity at room temperature. However, the very high value of lithium conductivity ($\sigma_{bulk} \approx 1 \times 10^{-3}$ Scm^{-1} at room temperature) reported some years ago in the literature for $La_{2/3-x}Li_{3x}TiO_3$,[1−5] with a perovskite-related structure (ABO_3), has renewed the interest for these crystalline materials as solid electrolytes for lithium batteries.

In this respect, a lot of effort has been dedicated to trying to improve the conducting properties of these titanates by substituting La and/or Ti by other metal ions. It would seem from this work that shortening of the A−O distances in the crystal structure by substituting La by a smaller rare earth metal such as Pr, Nd, or Sm decreases the ionic conductivity, because this reduces the bottleneck size which the Li^+ ions have to overcome.[3,6−7] On the contrary, a slightly higher value of the ionic conductivity has been reported for $(La_{0.5}Li_{0.5})_{0.95}Sr_{0.05}TiO_3$ ($\sigma_{300K} \approx 1.5 \times 10^{-3}$ Scm^{-1})[4] and $La_{0.517}Sr_{0.08}Li_{0.3}TiO_3$ ($\sigma_{300K} \approx 1.12 \times 10^{-3}$ Scm^{-1})[8] and this is attributed to Sr being bigger than La. Besides, it is believed that shortening of the B−O distances in the crystal structure can facilitate the ion motion, thereby increasing the ionic conductivity. This has been shown to be the case in $La_{0.5}Li_{0.5}Ti_{0.992}Ge_{0.008}O_3$ ($\sigma_{300K} \approx 1.12 \times 10^{-3}$ Scm^{-1}).[9] However, we believe that these results are not significant enough to really claim an improvement on the ionic conductivity in comparison with $La_{2/3-x}Li_{3x}\square_{1/3-2x}TiO_3$ ($\sigma_{300\ K} = 1.1\times 10^{-3}$ Scm^{-1} for $x = 0.1$ in ref 3; 1×10^{-3} Scm^{-1} for $x = 0.1$ in ref 4, and 1.4×10^{-3} Scm^{-1} for $x = 0.11$ in ref 5) as due to a size effect.

We have previously studied the conducting properties and crystal chemistry of the solid solutions $La_{2/3}Li_x\square_{1/3-x}Ti_{1-x}Al_xO_3$[10] and $La_{2/3-x}Sr_x\square_{1/3-x}Li_xTiO_3$,[11] where one could expect to still increase the conductivity values of the pristine system at high substitution levels, as this also corresponds to a high concentration of lithium ions; yet this does not seem to be the case. It actually appears that, apart from the size of the ions situated at the A and B positions of the crystal structure, the ratio between charge carriers and vacancies within the A sites is a crucial factor in controlling the ionic conductivity in these systems. In fact, the conductivity increases in parallel with the lithium content up to a value corresponding to a concentration of vacancies of about 8% for both solid solutions. This so being, and considering that the highest lithium conductivity obtained so far takes place in $La_{0.56}Li_{0.33}\square_{0.11}TiO_3$, we have studied

* To whom correspondence should be addressed. Phone: +34-91-394-4214. Fax: +34-91-394-4352. E-mail: sgmartin@quim.ucm.es.

(1) Belous, A. G.; Novitkaya, G. N.; Polyanetskaya, S. V.; Gornikov, Y. I. *Izv. Akad. Nauk SSSR, Neorg. Mater.* **1987**, *23* (*3*), 470.
(2) Inaguma, Y.; Liquan, C.; Itoh, M.; Nakamura, T. *Solid State Commun.* **1993**, *86* (*10*), 689.
(3) Kawai, H.; Kuwano, J. *J. Electrochem. Soc.* **1994**, *141*, L78.
(4) Inaguma, Y.; Liquan, C.; Itoh, M.; Nakamura, T. *Solid State Ionics* **1994**, *70−71*, 196.
(5) Inaguma, Y.; Itoh, M. *Solid State Ionics* **1996**, *86−88*, 257.
(6) Itoh, M.; Inaguma, Y.; Jung, W. H.; Liquan, C.; Nakamura, T. *Solid State Ionics* **1994**, *70/71*, 203.
(7) Morales, M.; West, A. R. *Solid State Ionics* **1996**, *91*, 33.
(8) Wang, G. X.; Yao, P.; Bradhurst, D. H.; Dou, S. X.; Lin, H. K. *J. Mater. Sci.* **2000**, *35*, 4289.
(9) Chum, H. T.; Kim, J. G.; Kim, H. G. *Solid State Ionics* **1998**, *107*, 153.
(10) Morata-Orrantia, A.; García-Martín, S.; Morán, E.; Alario-Franco, M. A. *Chem. Mater.* **2002**, *14*, 2871.
(11) Morata-Orrantia, A.; García-Martín, S.; Alario-Franco, M. A. *Chem. Mater.* **2003**, *15*, 363.

10.1021/cm0300563 CCC: $25.00
Published on Web 09/27/2003

Table 1. Molar Ratio of the Metal Ions for Three Samples Each of the Systems $La_{0.56}Li_{0.33+x}Ti_{1-x}Al_xO_3$ and $La_{0.56-x}Sr_xLi_{0.33+x}TiO_3$

		$La_{0.56}Li_{0.33+x}Ti_{1-x}Al_xO_3$		
	nominal composition	$La_{0.56}Li_{0.34}Ti_{0.99}Al_{0.01}O_3$	$La_{0.56}Li_{0.36}Ti_{0.97}Al_{0.03}O_3$	$La_{0.56}Li_{0.39}Ti_{0.94}Al_{0.06}O_3$
ICP	lithium	0.34 (2)	0.36 (2)	0.38 (2)
	aluminum	0.004 (2)	0.01(2)	0.03 (2)
	titanium	0.99 (1)	0.97 (1)	0.94 (1)
XRFS	lanthanum	0.57 (2)	0.57 (2)	0.55 (2)
	aluminum	0.013 (2)	0.04 (2)	0.065 (2)
	titanium	0.99 (1)	0.97 (1)	0.94 (1)
		$La_{0.56-x}Sr_xLi_{0.33+x}TiO_3$		
	nominal composition	$La_{0.55}Sr_{0.01}Li_{0.34}TiO_3$	$La_{0.53}Sr_{0.03}Li_{0.36}TiO_3$	$La_{0.52}Sr_{0.04}Li_{0.37}TiO_3$
ICP	lithium	0.35 (2)	0.36 (2)	0.38 (2)
	strontium	0.003 (2)	0.01 (2)	0.02 (2)
	titanium	1	1	1
XRFS	titanium	1	1	1
	lanthanum	0.55 (2)	0.53 (2)	0.52 (2)
	strontium	0.01 (2)	0.03 (2)	0.04 (2)

two new systems: $La_{0.56}Li_{0.33+x}\square_{0.11-x}Ti_{1-x}Al_xO_3$, in which the replacement of Ti by Al goes in parallel with an increase in lithium concentration, and $La_{0.56-x}Sr_xLi_{0.33+x}\square_{0.11-x}TiO_3$, in which La is substituted by Sr and Li. The aim of the work is to optimize the lithium ion/vacancy ratio together with a shortening of the B−O distances or an increasing of the A−O distances, so as to obtain a higher value of ionic conductivity. This is indeed what seems to happen and we have obtained the highest lithium conductivity reported to date in the La/Li titanates.

We present in here the stoichiometry range, crystal chemistry, and electrical properties of the above systems.

Experimental Section

Different compositions of the $La_{0.56}Li_{0.33+x}\square_{0.11-x}Ti_{1-x}Al_xO_3$ and $La_{0.56-x}Sr_xLi_{0.33+x}\square_{0.11-x}TiO_3$ systems were prepared from stoichiometric amounts of Li_2CO_3 (Merck 99%), $SrCO_3$ (Merck 99%), La_2O_3 (Aldrich 99.999%), TiO_2 (Aldrich 99.99%), and Al_3O_3 (Aldrich 99.99%). La_2O_3 was heated overnight at 1000 °C and TiO_2 and Al_2O_3 were heated at 700 °C prior to weighing. The mixtures were ground and then heated in platinum boats for 6 h for decarbonation. Afterward, the samples were reground, pelleted, covered with powder of the sample of the same composition to prevent lithia loss, and fired at 1150 °C for 12 h followed by further grinding, re-pelleting, and re-firing for another 12 h at 1275 °C. To study the evolution of the crystal structure with temperature, small amounts of sample were wrapped in Pt foil envelopes, annealed isothermally at different temperatures, and quenched to room temperature on a brass plate. Contrary to what happens in other systems[7,10,11,12] we did not notice differences between the X-ray diffraction patterns of the samples quenched from the synthesis temperature and the samples quenched from lower annealing temperatures. For this reason, we have used materials quenched from the synthesis temperature for this work. We have also prepared some oxides of the system $La_{2/3-x}Li_{3x}\square_{1/3-2x}TiO_3$ using the same procedure. In this case, samples quenched from the synthesis temperature were used as well.

The molar ratio of the metals in the compounds was determined by inductively coupled plasma mass spectroscopy (ICP-MS) and X-ray fluorescence spectroscopy (XRFS). For ICP-MS we used a Perkin-Elmer Elan 6000 with autosampler AS. To perform the ICP analysis, a solution protocol was optimized. Samples were treated with a mixture of nitric, hydrochloric, and hydrofluric acids in a 3:2:1 molar ratio at 150 °C in a CEM microwave furnace digestor (MDS-2000 model) with temperature and pressure sensors. Because of La^{3+} precipitation during the dilution of the acid solution, XRFS was used to analyze this cation using a Bruker S4 Explorer.

Crystalline phase identification and determination of the lattice parameters were carried out by powder X-ray diffraction (XRD) using a Philips X'PERT diffractometer with $CuK\alpha_1$ radiation, a curved Cu monochromator and the Philips X'ERT PEAPD software. The patterns were taken at step mode with a step size equal to 0.02 (2θ degrees) and time per step equal to 10 s.

The microstructure of the materials was characterized by selected area electron diffraction (SAED) and high-resolution transmission electron microscopy (HRTEM). Samples were ground in *n*-butyl alcohol and ultrasonically dispersed, and drops of the resulting suspension were deposited in carbon-coated grids. SAED studies were performed with an electron microscope JEOL 2000 FX (double tilt ± 45°) working at 200 kV, and HRTEM studies were done with an electron microscope JEOL 4000 FX (double tilt ± 25 °) working at 400 kV.

The electrical behavior of the materials has been studied by an impedance/gain phase analyzer Solartron 1255A with dielectric interface 1296. Pellets of about 13-mm diam and 2-mm thickness were prepared by pressing the powder samples and sintering them at 1200 °C. Electrodes were made by coating opposite pellet faces with platinum paste and heating them to 850 °C. Measurements were carried out in air on a heating cycle from 243 to 373 K and in a frequency range of 1×10^{-3} to 6.5×10^6 Hz.

Results and Discussion

Stoichiometric Range and Crystal Chemistry of the Solid Solutions $La_{0.56}Li_{0.33+x}\square_{0.11-x}Ti_{1-x}Al_xO_3$ and $La_{0.56-x}Sr_xLi_{0.33+x}\square_{0.11-x}TiO_3$. Single-phase materials are found for the solid solution $La_{0.56}Li_{0.33+x}\square_{0.11-x}Ti_{1-x}Al_xO_3$ over the composition range $0 \le x \le 0.06$ and for the system $La_{0.56-x}Sr_xLi_{0.33+x}\square_{0.11-x}TiO_3$ over $0 \le x \le 0.04$. $Li_2Ti_3O_7$ and Li_2TiO_3 were detected for compositions with $x > 0.06$ and $x > 0.04$, respectively. Chemical analyses appear in Table 1. We observed very good agreement between analytical and nominal compositions, so nominal compositions will be used in here.

The powder X-ray diffraction patterns of the materials of both systems show, besides the lines characteristic of the perovskite-type structure (cubic symmetry, lattice parameter $a_p = 3.8$ Å), the presence of very faint and wide reflections corresponding to $d \approx 7.6$ Å, $d \approx 3.4$ Å, and $d \approx 2.3$ Å, indicated by arrows in Figure 1 a and b. The intensity of these reflections does not increase with annealing of the samples at temperatures lower than

(12) Robertson, A. D.; García-Martín, S.; Coats, A.; West, A. R. *J. Mater. Chem.* **1995**, *5* (*9*), 1405.

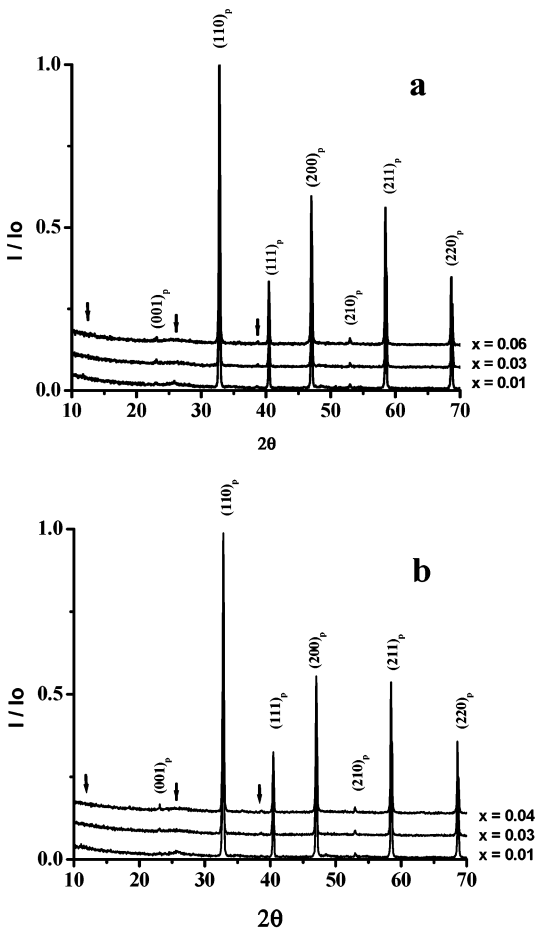

Figure 1. Powder XRD patterns of $La_{0.56}Li_{0.33+x}\square_{0.11-x}Ti_{1-x}Al_xO_3$ ($x = 0.01$, 0.02, and 0.06) (a) and of $La_{0.56-x}Sr_xLi_{0.33+x}\square_{0.11-x}TiO_3$ ($x = 0.01$, 0.03 and 0.04) (b) quenched from the temperature of synthesis. Miller indices of the cubic perovskite are indicated in the patterns.

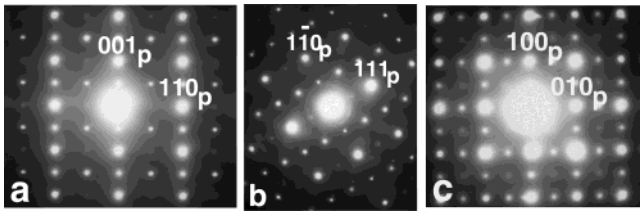

Figure 2. SAED patterns of $La_{0.56}Li_{0.36}\square_{0.08}Ti_{0.97}Al_{0.03}O_3$. Patterns along the $[\bar{1}\ 10]_p$ (a), $[\bar{1}\ \bar{1}2]_p$ (b), and $[001]_p$ (c) zone axes.

the synthesis temperature, contrary to what happens in both the pristine system[12] and related ones.[7,10−11]

Figure 2 shows three selected area electron diffraction patterns of the oxide with $x = 0.03$ of the $La_{0.56}Li_{0.33+x}\square_{0.11-x}Ti_{1-x}Al_xO_3$ system. The main reflections are indexed according to the ideal perovskite cell (p). Several extra reflections can be seen: $(001/2)_p$ reflections which double the *c*-axis in the pattern of the $[\bar{1}\ 10]_p$ zone axis; $(h/2\ h/2\ l/2)_p$ reflections in the three patterns and $(h/2\ 0\ 0)_p$ and $(0\ k/2\ 0)_p$ reflections, which apparently double the other two a_p and b_p lattice parameters, in the $[001]_p$ zone axis. All the materials prepared for these two systems $La_{0.56}Li_{0.33+\ x}\square_{0.11-x}Ti_{1-x}Al_xO_3$ and $La_{0.56-x}Sr_xLi_{0.33+x}\square_{0.11-x}TiO_3$ show similar electron diffraction patterns.

Therefore, both powder XRD and SAED patterns can be fully indexed only according to either a $\approx\sqrt{2}a_p \times \approx\sqrt{2}a_p \times \approx 2a_p$ or a $\approx 2a_p \times \approx 2a_p \times \approx 2a_p$ unit cell. In the case of the SAED pattern of the $[001]_p$ zone axis, if we consider the $\approx\sqrt{2}a_p \times \approx\sqrt{2}a_p \times \approx 2a_p$ cell, and the fact that $c \approx 2a_p$, the crystals should be twinned due to different orientations of the *c*-axis. Electron microscopy has been used to clarify which of these two cells is operating.

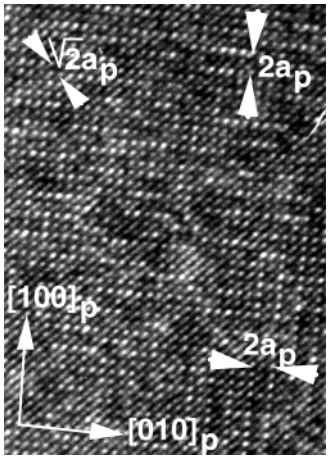

Figure 3. HRTEM image of $La_{0.56}Li_{0.36}\square_{0.08}Ti_{0.97}Al_{0.03}O_3$ corresponding to the $[001]_p$ zone axis.

Figure 3 shows a high-resolution transmission micrograph along the $[001]_p$ zone axis of $La_{0.56}Li_{0.36}\square_{0.08}Ti_{0.97}Al_{0.03}O_3$. The image corresponds to an average perovskite structure with $\approx\sqrt{2}a_p$ periodicity along the $[110]_p$ direction. Besides, microdomains (no bigger than two or three unit cells) with $\approx 2a_p$ periodicity alternating along either the $[100]_p$ or the $[010]_p$ directions are observed. These results indicate that the oxide has a distorted perovskite-type structure with a $\approx\sqrt{2}a_p \times \approx\sqrt{2}a_p \times \approx 2a_p$ unit cell and that the crystal is twinned as a consequence of the change of direction of the *c*-axis in the different microdomains. This type of microstructure is common to all materials studied in both solid solutions.

Distortion of the perovskite-type structure most probably occurs in these materials as a consequence of tilting of the [Ti/Al−O_6] octahedra to attain the appropiate A−O distances. Various tilt systems of the classification of the octahedra tilting in perovskites made by Glazer[13] and recently revised by Woodward[14,15] and by Howard and Stokes[16] give place to the so-called diagonal unit cell ($\approx\sqrt{2}a_p \times \approx\sqrt{2}a_p \times 2\approx a_p$). Ordering of the La^{3+}, Li^+, and vacancies along the *c*-axis can also occur. In fact, the presence of the $(001/2)_p$ reflection in the diffraction patterns would indicate cation ordering along the *c*-axis. This intensity maximum, which is rather strong in the electron diffraction patterns, is extremely weak and broad in the X-ray pattern. Microdomain formation, as shown by our electron micrographs, clearly causes the broadening of the superlattice reflections in the X-ray diffraction patterns.

Interestingly enough, the size of the diffracting domains does not seem to change with the annealing temperatures of the samples. However, we have reported the formation of big diffracting domains in other related systems[10,11] when annealing the samples at temperatures below the synthesis temperature. An

(13) Glazer, A. M. *Acta Crystallogr. B* **1972**, *28*, 3384.
(14) Woodward, P. M. *Acta Crystallogr. B* **1997**, *53*, 32.
(15) Woodward, P. M. *Acta Crystallogr. B* **1997**, *53*, 44.
(16) Howard, C. J.; Stokes, H. T. *Acta Crystallogr. B* **1998**, *54*, 782

Table 2. Lattice Parameters of $La_{0.56}Li_{0.33+x}Ti_{1-x}Al_xO_3$ and $La_{0.56-x}Sr_xLi_{0.33+x}TiO_3$

$La_{0.56}Li_{0.33+x}Ti_{1-x}Al_xO_3$

x	*a* (Å)	*b* (Å)	*c* (Å)	*V* (Å^3)
0	5.469 (5)	5.461 (4)	7.746 (4)	231.34 (2)
0.01	5.468 (4)	5.461 (4)	7.746 (6)	231.30 (2)
0.02	5.465 (3)	5.461 (4)	7.738 (5)	230.94 (2)
0.03	5.465 (3)	5.458 (4)	7.730 (5)	230.57 (2)
0.04	5.463 (3)	5.457 (4)	7.730 (6)	230.44 (2)
0.05	5.462 (4)	5.456 (3)	7.722 (5)	230.12 (2)
0.06	5.461 (4)	5.453 (3)	7.720 (5)	229.89 (2)

$La_{0.56-x}Sr_xLi_{0.33+x}TiO_3$

x	*a* (Å)	*b* (Å)	*c* (Å)	*V* (Å^3)
0.00	5.469 (5)	5.461 (4)	7.746 (5)	231.34 (2)
0.01	5.472 (4)	5.465 (3)	7.747 (4)	231.69 (2)
0.02	5.475 (2)	5.467 (3)	7.746 (5)	232.00 (1)
0.03	5.478 (5)	5.47 (3)	7.751 (3)	232.27 (1)
0.04	5.479 (4)	5.471 (2)	7.756 (4)	232.43 (1)

exception to this behavior seems to be the case of the materials with the highest lithium contents, in which microtwinning was always observed. As one could expect, the smaller the diffracting domains are, the wider are the superlattice reflections in the XRD patterns.

The X-ray patterns have been indexed using orthorhombic symmetry because, apart from giving slightly better according factors than the tetragonal cells, some weak splitting of the $(hh0)_p$ reflections far away from the origin is observed in the ED patterns. This splitting must be due to the slightly different size of the *a* and *b* lattice parameters and the concomitant twinning. Table 2 shows the lattice parameters and volume of the unit cell of materials corresponding to different *x* values for both solid solutions. Decreasing of the three parameters, and hence, of the volume, occurs in parallel with the introduction of Al^{3+} replacing Ti^{4+} and the accompanying Li^+ increasing. Therefore, the size of the cell is mainly affected by the size difference in the B-site (r(VI)Al^{3+} = 0.53 Å; r(VI)Ti^{4+} = 0.605 Å). On the contrary, increasing of the lattice parameters is observed when La^{3+} is substituted by Sr^{2+} and Li^+ due to the bigger size of the Sr^{2+} (r(VI)La^{3+} = 1.032 Å; r(VI)Sr^{2+} = 1.18 Å).

Electrical Properties of the $La_{0.56}Li_{0.33+x}\square_{0.11-x}Ti_{1-x}Al_xO_3$ ($0 \le x \le 0.06$) and $La_{0.56-x}Sr_xLi_{0.33+x}\square_{0.11-x}TiO_3$ ($0 \le x \le 0.04$) Systems. Bulk conductivity and grain-boundary conductivity values of all the oxides of both systems were obtained from the impedance complex diagrams at different temperatures. Figure 4 shows the plot of $\log\sigma_{bulk}$ vs $1000/T$ for three materials of the $La_{0.56}Li_{0.33+x}\square_{0.11-x}Ti_{1-x}Al_xO_3$ solid solution, and Table 3 gives the values of ionic conductivities (bulk and grain-boundary components) at 295 K and the activation energies of the conduction processes for all the oxides corresponding to this solid solution.

It can be seen that the activation energies are independent of the composition suggesting a common mechanism in all cases. The bulk conductivity increases with increasing lithium content up to the value 2.95×10^{-3} Scm^{-1} corresponding to $x = 0.03$. Therefore, the composition of the oxide with the highest ionic conductivity in the system is $La_{0.56}Li_{0.36}\square_{0.08}Ti_{0.97}Al_{0.03}O_3$, i.e., with 8% of vacancies within the A positions of the structure, as in the other related systems.[10-11]

A similar situation was measured in the $La_{0.56-x}Sr_xLi_{0.33+x}\square_{0.11-x}TiO_3$ system. Figure 5 shows the variation of $\log\sigma_{bulk}$ with $1000/T$ for three oxides and Table 4 gives

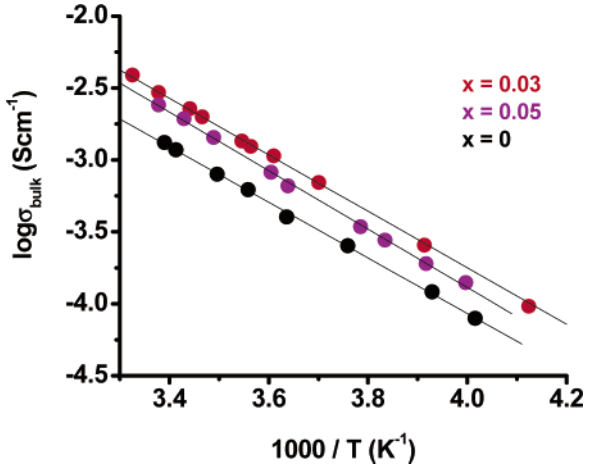

Figure 4. Plot of log σ_{bulk} vs $1000/T$ for $La_{0.56}Li_{0.33+x}\square_{0.11-x}Ti_{1-x}Al_xO_3$ (x = 0.00, 0.02, and 0.05).

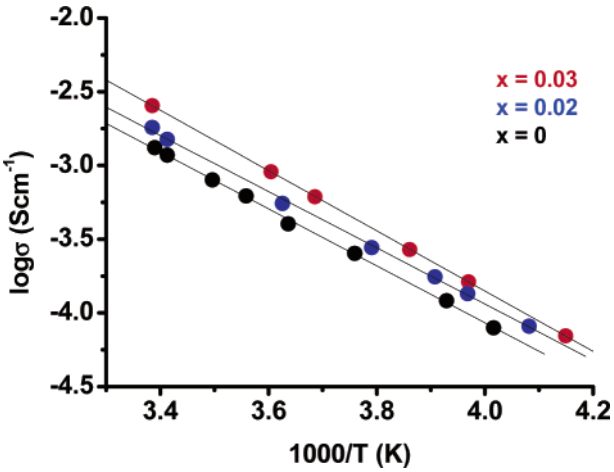

Figure 5. Plot of log σ_{bulk} vs $1000/T$ for $La_{0.56-x}Sr_xLi_{0.33+x}\square_{0.11-x}TiO_3$ (x = 0.00, 0.02, and 0.03).

the corresponding conductivity data. Again, the highest Li conductivity ($\sigma_{295K} = 2.54 \times 10^{-3}$ Scm^{-1}) is observed at the same value ($x = 0.03$) corresponding to 8% of A-vacancies; this is the oxide of composition $La_{0.53}Sr_{0.03}Li_{0.36}\square_{0.08}Ti\ O_3$.

This so being, we have re-studied the "classic" solid solution $La_{2/3-x}Li_{3x}\square_{1/3-2x}\ TiO_3$ for the oxides with compositions close to the optimum one, namely $x = 0.12$, 0.125, and 0.13. The conductivity values are of the same order as those reported for this system in the literature, but, once again, we obtain the highest value ($\sigma_{295K} = 1.9 \times 10^{-3}$ Scm^{-1}) for the oxide of composition corresponding to 8% ($x = 0.125$) of vacancies within the A cation sites. This value of conductivity is higher than any previous value given for the celebrated $La_{2/3-x}Li_{3x}\square_{1/3-2x}TiO_3$ system, yet it is substantially lower than those of our best results in the new systems $La_{0.56}Li_{0.33+x}\square_{0.11-x}Ti_{1-x}Al_xO_3$ and $La_{0.56-x}Sr_xLi_{0.33+x}\square_{0.11-x}TiO_3$.

Figure 6 shows the variation of the lithium conductivity at 295 K with the amount of vacancies (□) within the A sites of the structure for the three systems studied in this work and the other two previously reported.[10,11] Errors of the ionic conductivity values are of the same order of magnitude for all the systems (see Tables 3 and 4). It is pretty clear that the highest value in each solid solution corresponds to the materials with the 8% of A-site vacancies.

According to Table 2, the unit cell volume linearly decreases as Al replaces Ti in the structure of the

Table 3. Bulk and Grain-Boundary Conductivity values at 295 K and Activation Energies of $La_{0.56}Li_{0.33+x}Ti_{1-x}Al_xO_3$

x	σ_{bulk} (Scm^{-1})	σ_{bulk} (Scm^{-1})	$E_{a,bulk}$ (eV)	$E_{a,gb}$ (eV)
0	$1.32 \pm 0.2 \times 10^{-3}$	$5.01 \pm 0.3 \times 10^{-5}$	0.38 ± 0.006	0.45 ± 0.01
0.01	$2.26 \pm 0.3 \times 10^{-3}$	$5.76 \pm 0.2 \times 10^{-5}$	0.39 ± 0.004	0.44 ± 0.01
0.02	$2.82 \pm 0.4 \times 10^{-3}$	$4.59 \pm 0.4 \times 10^{-5}$	0.39 ± 0.007	0.49 ± 0.01
0.03	$2.95 \pm 0.3 \times 10^{-3}$	$4.94 \pm 0.3 \times 10^{-5}$	0.38 ± 0.003	0.48 ± 0.01
0.04	$2.62 \pm 0.3 \times 10^{-3}$	$2.55 \pm 0.4 \times 10^{-5}$	0.36 ± 0.004	0.42 ± 0.01
0.05	$2.41 \pm 0.3 \times 10^{-3}$	$1.31 \pm 0.2 \times 10^{-5}$	0.39 ± 0.005	0.43 ± 0.02
0.06	$1.66 \pm 0.2 \times 10^{-3}$	$2.15 \pm 0.3 \times 10^{-5}$	0.36 ± 0.009	0.48 ± 0.01

Table 4. Bulk and Grain-Boundary Conductivity Values at 295 K and Activation Energies of $La_{0.56-x}Sr_xLi_{0.33+x}TiO_3$

	σ_{bulk} (Scm^{-1})	σ_{bulk} (Scm^{-1})	$E_{a,bulk}$ (eV)	$E_{a,gb}$ (eV)
0	$1.32 \pm 0.2 \times 10^{-3}$	$5.10 \pm 0.3 \times 10^{-5}$	0.38 ± 0.006	0.45 ± 0.01
0.01	$1.35 \pm 0.2 \times 10^{-3}$	$5.43 \pm 0.3 \times 10^{-5}$	0.38 ± 0.004	0.45 ± 0.01
0.02	$1.98 \pm 0.3 \times 10^{-3}$	$4.82 \pm 0.2 \times 10^{-5}$	0.37 ± 0.006	0.41 ± 0.01
0.03	$2.54 \pm 0.3 \times 10^{-3}$	$4.73 \pm 0.3 \times 10^{-5}$	0.39 ± 0.006	0.42 ± 0.01
0.04	$1.97 \pm 0.2 \times 10^{-3}$	$5.01 \pm 0.3 \times 10^{-5}$	0.37 ± 0.007	0.43 ± 0.01

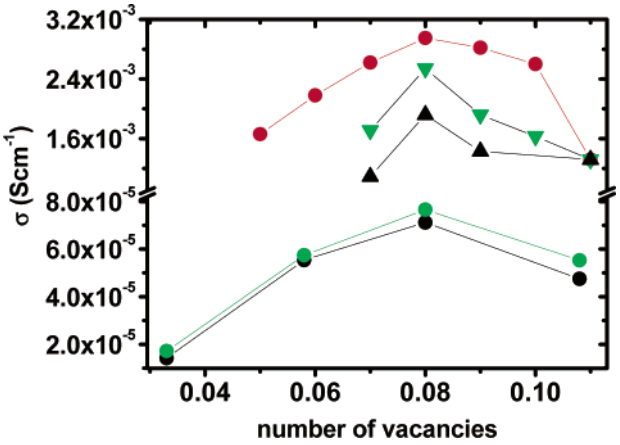

Figure 6. Plot of log $\sigma_{bulk\ 295K}$ vs amount of vacancies (□) within the A sites of the structure for $La_{0.56}Li_{0.33+x}\square_{0.11-x}Ti_{1-x}Al_xO_3$ (● red), $La_{0.56-x}Sr_xLi_{0.33+x}\square_{0.11-x}TiO_3$ (▼ green), $La_{2/3-x}Li_{3x}\square_{1/3-2x}TiO_3$ (▲ black), $La_{2/3}Li_x\square_{1/3-x}Ti_{1-x}Al_xO_3$ (● green), $La_{2/3-x}Sr_x\square_{1/3-x}TiO_3$ (● black).

$La_{0.56}Li_{0.33+x}\square_{0.11-x}Ti_{1-x}Al_xO_3$ system. On the contrary, it linearly increases when part of the La is substituted by Sr in the $La_{0.56-x}Sr_xLi_{0.33+x}\square_{0.11-x}TiO_3$ solid solution. Also, in both cases, the number of lithium ions (charge carriers) increases and the number of A-vacancies decreases. Although all these facts are initially beneficial for the conductivity, which does constantly increase, there is a clear maximum at 8% of vacancies of the A-site of the structure in every case. However, as we could expect, the concentration of charge carriers is a crucial factor to be taken into account to optimize the lithium conductivity. The lower conductivity of the two systems $La_{2/3}Li_x\square_{1/3-x}Ti_{1-x}Al_xO_3$[10] and $La_{2/3-x}Sr_x\square_{1/3-x}Li_xTiO_3$[11] is due to their lower amount of charge carriers. This is confirmed when comparing, for instance, $La_{0.67}Li_{0.25}\square_{0.08}Ti_{0.75}Al_{0.25}O_3$, with smaller unit cell parameters (a = 5.457 Å, b = 5.454 Å, c = 7.717 Å)[10] and lower conductivity ($\sigma_{295K} = 7.66 \times 10^{-5}$ Scm^{-1})[10] than $La_{0.56}Li_{0.36}\square_{0.08}Ti_{0.97}Al_{0.03}O_3$ (a = 5.465Å, b = 5.458 Å, c = 7.73 Å, and $\sigma_{295K} = 2.95 \times 10^{-3}$ Scm^{-1}). This is due to the latter sample having a higher number of charge carriers.

Conclusions

Study of the electrical properties of several lithium conducting titanates with a perovskite-related structure, led us to conclude that the maximum conductivity in each solid solution is achieved for the materials with ~8% of vacancies within the A-sites of the crystal structure. Therefore, to optimize lithium conductivity in this type of materials, the shortening of the B−O, or the increasing of the A−O, average distances has to be combined with an optimum ratio of charge carriers and A-cation vacancies.

Regarding the shortening of the B−O distances, we have found in the solid solution $La_{0.56}Li_{0.33+x}\square_{0.11-x}Ti_{1-x}Al_xO_3$, a composition for x = 0.03, corresponding to ~8% of vacancies, showing a conductivity as high as $\sigma = 2.95 \times 10^{-3}$ Scm^{-1} at 295 K. This is the highest lithium-ion conductivity value at room temperature ever reported in the literature for a crystalline material.[17] Besides, increasing the average A−O distances also seems to improve the ionic conductivity of the La/Li titanates, as we demonstrate in the $La_{0.56-x}Sr_xLi_{0.33+x}\square_{0.11-x}TiO_3$ system. In this case, the highest conductivity value ($\sigma_{295\ K} = 2.54 \times 10^{-3}$ Scm^{-1}) is obtained for the oxide of composition $La_{0.53}Sr_{0.03}Li_{0.36}\square_{0.08}Ti\ O_3$, which again corresponds to ~8% of vacancies within the A-cation sites.

The microstructure of these materials seems also to be an important factor affecting the ionic conductivity. In all the systems studied, the samples of highest conductivity have a microdomain texture instead of the big domains of ordering observed for some of the oxides annealed at temperatures lower than the synthesis temperature.[10−11] The size of the diffracting domains affects the profile of the XRD patterns,, i.e. microtwinning causes broadening of the superlattice reflections. All the studied materials have a $\approx\sqrt{2}a_p \times \approx\sqrt{2}a_p \times \approx 2a_p$ unit cell due to tilting of the [Ti/Al−O_6] octahedra suplemented with an ordering of the A-cations and A-vacancies (□) along the c axis.

Whether this particular charge carriers/vacancies ratio originates a specially favorable diffusion path for lithium is not yet clear. More work is in progress.

Acknowledgment. We thank the Spanish Ministery for Science and Technology (MAT 2001-371-CO4-04) for financial support and the Microscopy Centre Luis Bru and the X-ray diffraction C. A. I. from U. C. M. for technical assistance.

CM0300563

(17) Robertson, A. D.; West, A. R. *Solid State Ionics* **1997**, *104*, 1.